

# Low-redundancy Distillation for Continual Learning

Ruiqi Liu<sup>a,b</sup>, Boyu Diao<sup>a,b,\*</sup>, Libo Huang<sup>a</sup>, Zijia An<sup>a,b</sup>, Hangda Liu<sup>a,b</sup>, Zhulin An<sup>a,b</sup>,  
Yongjun Xu<sup>a,b</sup>

<sup>a</sup>*Institute of Computing Technology, Chinese Academy of Sciences, Beijing, 100190, China*

<sup>b</sup>*University of Chinese Academy of Sciences, Beijing, 100049, China*

---

## Abstract

Continual learning (CL) aims to learn new tasks without erasing previous knowledge. However, current CL methods primarily emphasize improving accuracy while often neglecting training efficiency, which consequently restricts their practical application. Drawing inspiration from the brain’s contextual gating mechanism, which selectively filters neural information and continuously updates past memories, we propose Low-redundancy Distillation (LoRD), a novel CL method that enhances model performance while maintaining training efficiency. This is achieved by eliminating redundancy in three aspects of CL: student model redundancy, teacher model redundancy, and rehearsal sample redundancy. By compressing the learnable parameters of the student model and pruning the teacher model, LoRD facilitates the retention and optimization of prior knowledge, effectively decoupling task-specific knowledge without manually assigning isolated parameters for each task. Furthermore, we optimize the selection of rehearsal samples and refine rehearsal frequency to improve training efficiency. Through a meticulous design of distillation and rehearsal strategies, LoRD effectively balances training efficiency and model precision. Extensive experimentation across various benchmark datasets and environments demonstrates LoRD’s superiority, achieving the highest accuracy with the lowest training FLOPs.

## Keywords:

Continual Learning, Lifelong Learning, Catastrophic Forgetting, Knowledge Distillation, Experience Replay

---

---

\*Corresponding author

## 1. Introduction

Continual learning is the process where a machine learning model adapts to new data while retaining old knowledge in a dynamic environment [1]. Within CL, Deep Neural Networks face the challenge of *Catastrophic Forgetting* [2], an issue where the acquisition of new knowledge can lead to a rapid erosion of previously learned knowledge [3]. Although recent methods mainly focus on this forgetting issue, deploying CL on edge devices, such as the NVIDIA Jetson TX2 [4], is crucial for achieving real-time edge intelligence. When deploying CL on resource-constrained devices, learning efficiency becomes equally important. However, prior CL works have often overlooked the inherent efficiency of the algorithms themselves, focusing primarily on improving accuracy.

Various methods have been implemented to mitigate *Catastrophic Forgetting*. Architecture based methods [5] allocate distinct parameters for each task to decouple task-specific knowledge. Regularization based methods [6] restrict updates to crucial parameters or distill the entire model. Rehearsal based methods [7] prevent forgetting by retaining samples from previous tasks. Although these methods enhance model performance, they introduce considerable computational overhead during training, limiting their practical application—even underperforming the simplest rehearsal-based method ER [8] in real-world applications [9]. A limited number of studies explore training efficiency in CL [10]. Among these, SparCL [11] reduces the FLOPs required for model training by implementing dynamic weight and gradient masks, along with selective sampling of crucial data. These methods accelerate the training process through pruning and sparse training but do not achieve joint optimization with precision, resulting in mediocre performance.

Knowledge distillation and sample rehearsal have been proven to be the most effective methods for mitigating *catastrophic forgetting* [12]. However, they face three significant challenges: (1) the effectiveness of the distillation methods is compromised because the teacher model cannot encode all useful information efficiently [13]; (2) rehearsal-based methods suffer from an inherent imbalance between samples of previous and current tasks, leading to model updates biased toward the current task (*i.e.*

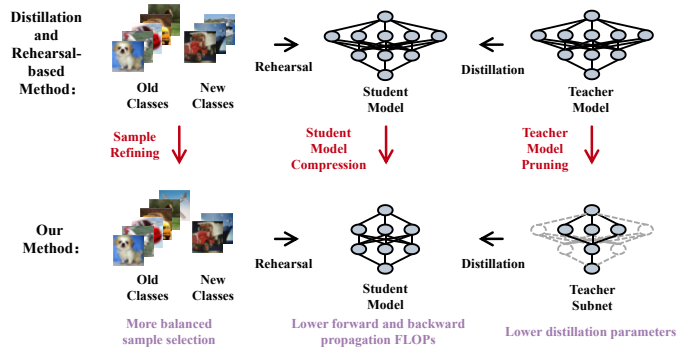


Figure 1: Overview of LoRD. We employ Sample Refining to achieve a more balanced sample selection, Student Model Compression to reduce forward and backward propagation FLOPs, and Teacher Model Pruning to minimize distillation parameters. Each of these techniques targets redundancy reduction, leading to improved accuracy and enhanced training efficiency.

recency bias [14]); (3) both methods introduce substantial computational overhead, resulting in poor performance in real-world applications [15]. In contrast, the human brain employs a gating mechanism to filter redundant neural information based on context, allowing for efficient retention and updating of past memories [16]. Drawing inspiration from this biological mechanism, we aim to address these three challenges by eliminating redundancy in both distillation and rehearsal-based methods. Our goal is to achieve state-of-the-art (SOTA) accuracy while reducing training FLOPs, ultimately improving efficiency compared to ER, which has demonstrated superior performance in real-world applications and serves as a critical benchmark for evaluating efficiency [9].

To this end, we propose the Low-redundancy Distillation (LoRD), a novel CL method that achieves collaborative optimization of accuracy and training efficiency by eliminating redundancy in the learning process. Inspired by the human brain’s gating mechanism, which filters out redundant information to efficiently retain and update past memories, LoRD reduces redundancy in the CL process across three aspects: the student model, the teacher model, and replay samples, as shown in Fig. 1. Specifically, we compress the number of learnable parameters in the student model, allocating parameters at each task boundary to ensure its plasticity. Simultaneously, we save the student model from the last task as the teacher model for the current task. The teacher

model is pruned to create a teacher subnet, and the subnet with an identical structure in the student model is distilled to maintain its stability. This distillation method not only reduces redundancy in the CL distillation process but also allows non-distilled weights to adapt to new tasks while distilled weights retain knowledge from previous tasks. LoRD provides a new mechanism for decoupling task-specific knowledge, effectively addressing the issue of recency bias. To help the teacher model efficiently encode and optimize previous knowledge, consistent with DER [7], we retain the logits of previous samples for distillation and utilize two collaborative distillation methods. Furthermore, we optimize the selection of rehearsal samples to further reduce redundancy in the rehearsal process, thereby boosting the model’s performance and training efficiency. Aligned with the brain’s gating mechanism, LoRD enables CL models to efficiently filter and preserve crucial knowledge, optimizing it in subsequent learning processes. LoRD achieves SOTA accuracy with lower training FLOPs than the ER method, facilitating its application in real-world scenarios.

In summary, our contributions are as follows:

- Inspired by the human brain’s gating mechanism, which efficiently filters out redundant information to retain and update past memories, we propose LoRD, a novel CL method that optimizes model performance while maintaining training efficiency by eliminating redundancy in three aspects of CL: student model redundancy, teacher model redundancy, and rehearsal sample redundancy.
- We explore the synergy between distillation and rehearsal methods, and as a result, LoRD effectively decouples task-specific knowledge without manually assigning isolated parameters for each task.
- Experiments conducted in both cloud and edge environments have demonstrated that LoRD outperforms SOTA methods, achieving up to a 3.8% increase in accuracy while reducing training FLOPs by 12% compared to the ER method.

## 2. Related Work

*Effective Continual Learning.* Effective continual learning aims to mitigate *catastrophic forgetting* and is typically classified into three main categories: regularization-based methods, architecture-based methods, and rehearsal-based methods.

*Regularization-based Methods* [17] limit the drift of crucial network parameters in previous tasks. The distillation methods [18], which are also considered regularization methods, constrain the new model’s output for the original task to be similar to that of the old model by designating the previous model snapshot as the teacher. However, the teacher model may encounter forgetting problems, a challenge effectively tackled by LoRD through the synergistic utilization of two distinct types of distillation losses.

*Architecture-based Methods* [19] allocate distinct parameter sets for each task. Certain architecture-based methods [5] focus on freezing or pruning subnets to decouple knowledge. LoRD enhances the model’s stability through distillation and sample replay, avoiding the manual selection and freezing of crucial weights, thereby promoting the model’s forward transfer capability [20]. Moreover, LoRD improves the model’s plasticity by assigning parameters to the student model instead of persistently pruning it.

*Rehearsal-based Methods* [21] employ a replay buffer to store and periodically revisit data from previous tasks, preserving knowledge and mitigating forgetting. ER [8] enhances learning by interleaving current task samples with those from previous tasks. Building upon this, DER [7] further augments the learning process by storing past model logits and utilizing these logits for distillation. Although rehearsal-based methods are acknowledged as the current state-of-the-art [7], their effectiveness can be severely impacted if the buffer size is small. Additionally, prior studies [9] have found that the training FLOPs of CL methods are crucial for real-world applications because long training times before deployment are impractical. Consequently, the ER method often achieves the best performance in practical settings due to its low training FLOPs. LoRD improves training efficiency by eliminating redundancy, achieving SOTA performance with lower training FLOPs than ER.

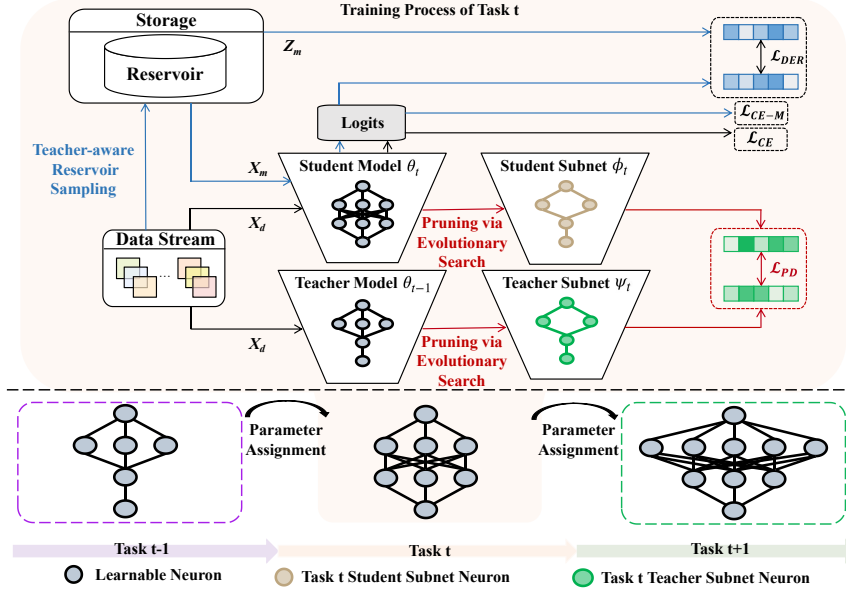


Figure 2: The main framework of LoRD. **Above the dashed line:** During the training of each task, we prune the teacher model into a teacher subnet and distill the student subnet that has the same structure as the teacher subnet. Additionally, we propose Teacher-aware Reservoir Sampling to optimize the selection of replay samples. **Below the dashed line:** We compress the number of learnable parameters in the student model to reduce redundancy. At each task boundary, we assign these learnable parameters to the student model to ensure its plasticity.

*Efficient Continual Learning.* The aim of efficient continual learning [22] is to enhance the efficiency of CL by optimizing training speed, memory usage, and computational resource utilization. SparCL [11] stands out among various methods by reducing the model’s training FLOPs through the utilization of dynamic weight and gradient masks, along with selective sampling of crucial data. In contrast to conventional efficient CL methods that primarily focus on optimizing training efficiency, LoRD aims to maximize model performance while maintaining training efficiency by eliminating redundancy in the learning process. Furthermore, our method can be combined with efficient CL methods, as demonstrated in Sec. 4.7.

### 3. Method

We describe a novel CL method, LoRD (as shown in Fig. 2), in this section. LoRD aims to optimize model performance while maintaining training efficiency by eliminating redundancy in the learning process. Before going into in-depth, we first clarify the problem setting.

#### 3.1. Problem Setting

The CL problem involves sequentially learning  $T$  tasks from a dataset, where each task  $t$  has a training set  $\mathcal{D}^t = \{(x_i^t, y_i^t)\}_{i=1}^{N_t}$  with  $N_t$  i.i.d. samples represented by pairs  $(x_i^t, y_i^t)$ . The objective of CL is to perform sequential training while preserving the performance of previous tasks. This objective can be achieved by learning a working model  $f_\theta(\cdot)$  that minimizes classification loss across all tasks  $t = \{1, \dots, T\}$  [7]:

$$\mathcal{L}_{\text{CE}} = \mathbb{E}_{(x^t, y^t) \sim \mathcal{D}^t} \ell(\sigma(f_\theta(x)), y), \quad (1)$$

where  $\ell(\cdot, \cdot)$  represents cross-entropy loss,  $\sigma(\cdot)$  is the softmax function. Due to the unavailability of historical task data, rehearsal-based methods incorporate a replay buffer  $\mathcal{M} = (x_i, y_i)_{i=1}^{\mathcal{B}}$ . This buffer, with a constant size  $\mathcal{B}$ , facilitates adapting to new tasks and retaining knowledge from previous tasks. During the training process, we replay samples from the buffer based on ER [8]. The classification loss on memory can be formulated as:

$$\mathcal{L}_{\text{CE-M}} = \mathbb{E}_{(x, y) \sim \mathcal{M}} \ell(\sigma(f_\theta(x)), y). \quad (2)$$

Furthermore, the distillation methods utilize logit matching [23] to efficiently reduce changes in the crucial parameters of the model. Among these methods, DER [7] stores the output logits  $z \triangleq f_{\theta'}(x)$  of previous models and utilizing them for distillation, where  $t$  indicates the time of memory insertion:

$$\mathcal{L}_{\text{DER}} = \mathbb{E}_{(x, z) \sim \mathcal{M}} \|f_\theta(x), z\|_2^2, \quad (3)$$

and DER++ [7] further replays both logits and ground-truth labels:

$$\mathcal{L}_{\text{DER++}} = \beta_1 \mathcal{L}_{\text{CE-M}} + \beta_2 \mathcal{L}_{\text{DER}}, \quad (4)$$

where  $\beta_1$  and  $\beta_2$  are weighting factors.

### 3.2. Low-redundancy Distillation

The human brain possesses a gating mechanism that filters out redundant neural information based on context and continuously updates past memories. Therefore, we propose pruning through evolutionary search and compression via cosine annealing in the distillation process to reduce redundancy. In LoRD, we use the working model from the last task as the teacher model  $f_{\theta_{t-1}}(\cdot)$  for the current task, while the current model serves as the student model  $f_{\theta_t}(\cdot)$ . By filtering out redundancies, LoRD enables the teacher model to consistently update and preserve essential knowledge.

#### 3.2.1. Student Model Compression

We reduce the redundancy of the student model by compressing its learnable parameters. Instead of directly updating the entire student model, we incrementally allocate the learnable parameters. We segment the filters in each layer into  $G$  groups [24]. Subsequently, at the boundary of the  $t$ -th task, we select  $s_t$  groups of filters to assign as learnable filters for the student model. The allocation of parameters is crucial, as we need to leave a room for future tasks while fully learning the current task. For initial task learning, LoRD employs knowledge distillation to concentrate previous task knowledge within the distilled student subnet, while enabling non-distilled parameters to rapidly adapt to new tasks. However, with increasing task numbers, the distilled student subnet demonstrates gradual forgetting of prior knowledge, while replay methods tend to utilize more non-distilled parameters for old knowledge consolidation, consequently impairing model plasticity. To address this, LoRD incorporates a cosine annealing algorithm for parameter allocation, thereby assigning supplementary parameters to subsequent tasks to maintain plasticity. This compression method allows the student model to ensure stability through replay and distillation mechanisms while gaining additional parameters to enhance plasticity, thus effectively addressing catastrophic forgetting with incremental tasks while improving training efficiency through optimized parameter utilization. For the  $t$ -th task boundary, the  $s_t$  is determined as follows:

$$s_t = \frac{1}{2}r \left( 1 + \cos \left( \frac{t \times \pi}{N} \right) \right), \quad (5)$$

where  $0 \leq t \leq N - 1$  and  $N$  is the expected number of tasks for CL. To fully leverage the capacity of the student model, all parameters should be learnable upon reaching the  $N$ -th task boundary. The value of  $r$  is thus determined as follows:

$$r = \frac{2G}{\sum_{t=0}^{N-1} \left(1 + \cos\left(\frac{t\pi}{N}\right)\right)}, \quad (6)$$

and the number of learnable filter groups  $g_t$  for the  $t$ -th task can be calculated as follows:

$$g_t = \sum_{i=0}^{t-1} s_i = \frac{G \sum_{i=0}^{t-1} \left(1 + \cos\left(\frac{i\pi}{N}\right)\right)}{\sum_{i=0}^{N-1} \left(1 + \cos\left(\frac{i\pi}{N}\right)\right)}. \quad (7)$$

When the number of tasks  $N$  is unknown (i.e., when  $N$  approaches infinity),  $g_t$  becomes infinitesimally small. Therefore, we constrain  $s_t$  to have a minimum value of 1. Our parameter allocation method controls the learnable parameters in the student model through structured pruning, which achieves model compression by systematically removing entire structural components rather than applying parameter masking. Through this parameter allocation process, LoRD dynamically generates authentic student subnets, thereby ensuring reduced computational complexity during both forward and backward propagation.

### 3.2.2. Teacher Model Pruning

We utilize the student model from the previous task as the teacher model for the current task and prune it to reduce redundancy. In contrast to conventional pruning methods [11] that consider weight importance, we design pruning strategies based on three perspectives: (1) We prune filters to obtain a teacher subnet to enhance distillation efficiency. (2) The pruned teacher subnet should have similar logits outputs to the teacher network, and (3) the redundancy of the teacher subnet should be reduced, meaning the number of parameters should be small. We formalize the problem as follows:

$$\operatorname{argmin}_{\psi_t} \exp\left(\frac{|\psi_t|}{|\theta_{t-1}|}\right) \|f_{\theta_{t-1}}(x) - f_{\psi_t}(x)\|_2^2, \quad (8)$$

where  $f_{\psi_t}(\cdot)$  is the pruned teacher subnet and  $|\psi_t|$  represents the number of its parameters.  $\exp\left(\frac{|\psi_t|}{|\theta_{t-1}|}\right)$  is utilized to control the size of the parameters. Consistent with [24], we conduct an evolutionary search [25] to get a teacher subnet that minimizes Eq. 8.

We define the width  $g_t$  of the current student model as the overall search space for the evolutionary search. To construct the initial population of candidate subnets, we randomly select a width value no greater than  $g_t$  for each layer of the network architecture. Finally, we employ evolutionary search based on Eq. 8 to identify the optimal teacher subnet. In the evolutionary search for the teacher subnet, instead of using masks to record which neurons are activated, we record the width of each layer and obtain the teacher subnet by pruning the less important filters according to the predefined width. The search process completes within a minute.

During the distillation stage, the teacher subnet and the student model are not directly utilized. Instead, we prune a student subnet with a structure identical to the teacher subnet from the student model and perform distillation between these two subnets. We compute the following loss term:

$$\mathcal{L}_{\text{PD}} = \mathbb{E}_{(x,y) \sim \mathcal{D}} \|f_{\phi_t}(x) - f_{\psi_t}(x)\|_2^2, \quad (9)$$

where  $f_{\phi_t}(\cdot)$  is the pruned student subnet. By employing Eq. 9, LoRD allows non-distilled weights to adapt to new tasks, while distilled weights retain knowledge from previous tasks. This method decouples task-specific knowledge and addresses the issue of recency bias. Furthermore, We employ two types of distillation losses, Eq. 3 and Eq. 9. Relying solely on Eq. 3 would prevent the effective update of prior knowledge, leading to incomplete encoding of useful information. Conversely, relying solely on Eq. 9 would subject the teacher model to forgetting. Through the combined application of both distillation functions, the teacher network can efficiently encode useful knowledge and improve distillation performance.

### 3.3. Teacher-aware Reservoir Sampling

Here, we provide the sampling algorithm for the TRS. This algorithm effectively manages the memory buffer based on the knowledge retention capabilities of the teacher subnet, ensuring that valuable experiences are retained. Some prior CL works improve reservoir sampling by selecting informative examples to construct the replay buffer [26]. However, they do not consider computing resource utilization [27], resulting in excessive computational costs. To enhance replay efficiency while minimiz-

---

**Algorithm 1** TRS Algorithm

---

**Input:** Memory Buffer  $\mathcal{M}$ , Memory Budget  $\mathcal{B}$ , Number of seen examples  $N$ , Teacher subnet parameter quantity  $|\psi_t|$ , Student model parameter quantity  $|\theta_t|$ , Selected example  $(x, y)$ .

**if**  $\mathcal{B} > N$  **then**

$\mathcal{M}[N] \leftarrow (x, y)$  ▷ Memory is not full

**else**

$k = \text{randomInteger}(\text{min} = 0, \text{max} = N)$

$i = \text{random}(\text{min} = 0, \text{max} = 1)$

**if**  $i < \exp(-\alpha \frac{|\psi_t|}{|\theta_t|})$  **then**

**if**  $k < \mathcal{B}$  **then**

$\mathcal{M}[k] \leftarrow (x, y)$  ▷ Select a sample to remove

**end if**

**end if**

**end if**

**return**  $\theta$

---

ing additional computational burden, we propose Teacher-aware Reservoir Sampling (TRS) method. Due to the use of two types of distillation losses, the purpose of replaying samples has shifted from preventing model forgetting to helping teacher networks better encode knowledge from old tasks. Based on this, we reduce the likelihood of storing the current sample based on the knowledge retention capabilities of the teacher subnet. The probability of storing the  $k$ -th ( $k > \mathcal{B}$ ) sample in the buffer is denoted as  $p(x_k)$  and the calculation of  $p(x_k)$  can be performed as follows:

$$p(x_k) = \exp(-\alpha \frac{|\psi_t|}{|\theta_t|}) \frac{\mathcal{B}}{k}, \quad (10)$$

where  $\alpha$  is a weighting factor and we assess the knowledge retention capabilities of the teacher subnet based on their size. The sampling process for the TRS algorithm is detailed in Algorithm 1, where both indices  $i$  and  $k$  are sampled from a uniform

---

**Algorithm 2** The training algorithm of the LoRD

---

**Require:** Data stream  $\mathcal{D}$ , Buffer  $\mathcal{M}$ , Model weight  $\theta$

```
1: for  $t = 0, \dots, T$  do
2:   Assign learnable parameters by Eq. 7
3:   while Training one task do
4:      $(X_d, Y_d) \leftarrow \text{sample}(\mathcal{D})$ 
5:     Calculate  $\mathcal{L}_{\text{CE}}$  and  $\mathcal{L}_{\text{PD}}$  by Eq. 1 and Eq. 9
6:      $(X_m, Y_m, Z_m) \leftarrow \text{sample}(\mathcal{M})$ 
7:     Calculate  $\mathcal{L}_{\text{DER++}}$  and  $\mathcal{L}$  by Eq. 4 and Eq. 11
8:      $\theta \leftarrow \theta - \eta \nabla_{\theta} \mathcal{L}$ 
9:      $\mathcal{M} \leftarrow \text{TRS}(\mathcal{M}, (X_d, Y_d))$ 
10:   end while
11:   Prune the teacher model for the next task by Eq. 8
12: end for
13: return  $\theta$ 
```

---

distribution<sup>1</sup>. Furthermore, we delve deeper into examining the correlation between rehearsal frequency (RF) and distillation. Within the DER method, each batch comprises half the samples from the new task and half the samples from the buffer. Notably, the inclusion of the teacher model has resulted in a decreased requirement for replay samples, enabling LoRD to adjust RF based on the desired trade-off between accuracy and efficiency. We conduct a comprehensive exploration study on RF, detailed in Sec. 4.7, to further underscore our method’s effectiveness.

### 3.4. The Overall Loss

In summary, the total training objective for LoRD can be expressed by:

$$\mathcal{L} = \mathcal{L}_{\text{CE}} + \lambda \mathcal{L}_{\text{PD}} + \mathcal{L}_{\text{DER++}}, \quad (11)$$

where  $\lambda$  is a weighting factor and the cross-entropy loss  $\mathcal{L}_{\text{CE}}$  focuses on learning the current data;  $\mathcal{L}_{\text{PD}}$  assists the model in preserving and updating essential knowledge.;

---

<sup>1</sup>We provide more details about TRS in Appendix A.

$\mathcal{L}_{\text{DER}++}$  helps teachers model better encoding knowledge.

We provide a detailed description of the overall training procedure of LoRD in Algorithm 2. Upon the arrival of new data, our method involves the following steps: Firstly, we compute the overall objective  $\mathcal{L}$ . Subsequently, we update the weights in the compressed student model through gradient descent. Finally, we utilize TRS to update the buffer.

## 4. Experiments

### 4.1. Dataset and Hardware

We conduct experiments on commonly used public datasets, including Split CIFAR-10 (S-CIFAR-10) [7], Split CIFAR-100 (S-CIFAR-100) [28], and Split Tiny ImageNet (S-Tiny-ImageNet) [29]. The Split CIFAR-10 dataset comprises 5 tasks, each containing 2 classes, while the Split CIFAR-100 dataset consists of 20 tasks, each containing 5 classes. The Split Tiny ImageNet dataset is created by dividing the original Tiny ImageNet dataset [30], which includes 200 classes, into 10 tasks, with each task consisting of 20 classes. We conduct comprehensive experiments utilizing the NVIDIA GTX 2080Ti GPU paired with the Intel Xeon Gold 5217 CPU, as well as the NVIDIA Jetson TX2, boasting 8 GB LPDDR4 Main Memory and 32 GB of eMMC Flash memory.

### 4.2. Evaluation Metrics

We use the following two metrics to measure the performance of various methods:

$$ACC_t = \frac{1}{t} \sum_{\tau=1}^t R_{t,\tau} \quad (12)$$

$$FF_t = \frac{1}{t-1} \sum_{j=1}^{t-1} \max_{i \in \{1, \dots, t-1\}} (R_{i,j} - R_{t,j}), \quad (13)$$

We denote the classification accuracy on the  $\tau$ -th task after training on the  $t$ -th task as  $R_{t,\tau}$ . A higher ACC value indicates superior model performance, while a lower FF value signifies enhanced anti-forgetting efficacy of the model. We employ the Split CIFAR-10, Split CIFAR-100, and Split Tiny ImageNet datasets to validate the effectiveness of

our method in both Task Incremental Learning (Task-IL) and Class Incremental Learning (Class-IL) [18] settings. In the simplest testing setup, it is assumed that the identity of each incoming test instance is known, which is referred to as Task-IL. If, during CL inference, the subset of classes for each sample is not recognized, the scenario transitions to a more complex Class-IL setting. This research primarily focuses on the more intricate Class-IL setting, while the performance of Task-IL is used solely for comparative analysis.

### 4.3. Baselines.

We compare LoRD with several representative baseline methods, including three regularization-based methods: oEWC [31], SI [32] and LwF [17], as well as eleven rehearsal-based methods: ER [8], GEM [20], A-GEM [28], iCaRL [33], GSS [27], HAL [34], DER [7], DER++ [7],  $Co^2L$  [35], ER-ACE [36] and SCoMMER [37]. It’s important to highlight that many rehearsal-based methods also integrate regularization. In our evaluation, we incorporate two non-continual learning baselines: SGD (lower bound) and JOINT (upper bound).

### 4.4. Implementation Details

For the CIFAR and Tiny ImageNet datasets, we adopt a standard ResNet18 [38] architecture without pretraining as the baseline, following the method taken in [33]. We expand the Mammoth CL repository in PyTorch [7], and we employ random crops and horizontal flips as data augmentation techniques for both examples from the current task and the replay buffer. All models are trained using the Stochastic Gradient Descent (SGD) optimizer and the batch size is fixed at 32. The details of other hyperparameters can be found in Appendix B and Appendix C. In the Split Tiny ImageNet setting, the models are trained for 100 epochs. As for the Split CIFAR-10 and Split CIFAR-100 settings, the models are trained for 50 epochs in each phase. For rehearsal-based methods, each batch comprises a combination of half the samples from the new task and half the samples from the buffer. When the RF is set to 1/2, the calculation of the loss on the buffer for backpropagation will occur only once every two batches. To ensure robustness, all experiments are repeated 10 times with different initializations, and the results are averaged across the runs.

Table 1: Classification results for S-CIFAR-10 dataset. The highest results are marked in bold.

Method	Class-IL		Task-IL	
	200	500	200	500
JOINT	92.20±0.15		98.31±0.12	
SGD	19.62±0.05		61.02±3.33	
GEM [20]	25.54±0.76	26.20±1.26	90.44±0.94	92.16±0.69
iCaRL [33]	49.02±3.20	47.55±3.95	88.99±2.13	88.22±2.62
ER [8]	44.79±1.86	57.74±0.27	91.19±0.94	93.61±0.27
A-GEM [28]	20.04±0.34	22.67±0.57	83.88±1.49	89.48±1.45
GSS [27]	39.07±5.59	49.73±4.78	88.80±2.89	91.02±1.57
DER [7]	61.93±1.79	70.51±1.67	91.40±0.92	93.40±0.39
DER++ [7]	64.88±1.17	72.70±1.36	91.92±0.60	93.88±0.50
HAL [34]	32.36±2.70	41.79±4.46	82.51±3.20	84.54±2.36
$Co^2L$ [35]	65.57±1.37	74.26±0.77	93.43±0.78	95.9±0.26
ER-ACE [36]	63.22±1.44	71.85±0.52	92.28±0.34	94.22±0.18
SCoMMER [37]	69.19±0.61	74.97±1.05	93.20±0.10	94.36±0.06
<b>LoRD (Ours)</b>	<b>70.16±1.23</b>	<b>75.68±0.53</b>	93.94±0.30	94.97±0.29

#### 4.5. Experimental Results

*Buffer-based Settings.* Tab. 1 and Tab. 2 present the ACC of all tasks after training. The results demonstrate that LoRD achieves superior performance across different experimental settings. In Class-IL, LoRD outperforms the second-best method by up to 3.8%. Conventional rehearsal-based methods predominantly depend on replay samples to retain knowledge from previous tasks. Conversely, our method utilizes low-redundancy distillation to decouple task-specific knowledge, allowing LoRD to achieve superior performance.

*Buffer-free Settings.* The results, as illustrated in Fig. 3, present the ACC across all tasks following training. Traditional regularization-based methods calculate parame-

Table 2: Classification results for S-Tiny-ImageNet dataset. The highest results are marked in bold.

Method	Class-IL		Task-IL	
	200	500	200	500
JOINT	59.99±0.19		82.04±0.10	
SGD	7.92±0.26		18.31±0.68	
GEM [20]	12.56±0.41	14.92±1.06	39.28±0.77	48.98±0.89
iCaRL [33]	7.53±0.79	9.38±1.53	28.19±1.47	31.55±3.27
ER [8]	8.49±0.16	9.99±0.29	38.17±2.00	48.64±0.46
A-GEM [28]	8.07±0.08	8.06±0.04	22.77±0.03	25.33±0.49
GSS [27]	14.78±0.87	18.23±1.35	38.22±0.98	50.47±0.72
DER [7]	11.87±0.78	17.75±1.14	40.22±0.67	51.78±0.88
DER++ [7]	10.96±1.17	19.38±1.41	40.87±1.16	51.91±0.68
HAL [34]	13.07±0.57	16.95±0.89	39.95±1.12	51.36±0.58
$Co^2L$ [35]	13.88±0.4	20.12±0.42	42.37±0.74	53.04±0.69
ER-ACE [36]	13.82±0.03	21.16±0.15	45.09±0.25	54.39±0.35
SCoMMER [37]	9.50±0.86	17.85±0.35	35.95±3.02	52.85±0.67
<b>LoRD (Ours)</b>	<b>17.68±1.06</b>	<b>24.01±0.36</b>	<b>47.68±1.23</b>	<b>50.08±0.74</b>

ter importance based on prior tasks and maintain these critical parameters unaltered. However, as new tasks arrive, the significance of these parameters evolves. In contrast, LoRD adapts and updates critical parameters during the learning process, continuously optimizing performance and achieving superior results across various scenarios. In Class-IL, our method surpasses the suboptimal method in ACC on S-CIFAR-10 and S-Tiny-ImageNet datasets by 8.8% and 6.5%, respectively.

*Settings with Unknown Task Numbers.* To evaluate the performance of LoRD when the number of tasks  $N$  is unknown, we test various methods on the S-CIFAR-100 dataset, which consists of 20 tasks. The results, presented in Fig. 4, show that LoRD achieves the highest Class-IL accuracy, even when  $N$  is unknown. This demonstrates that LoRD

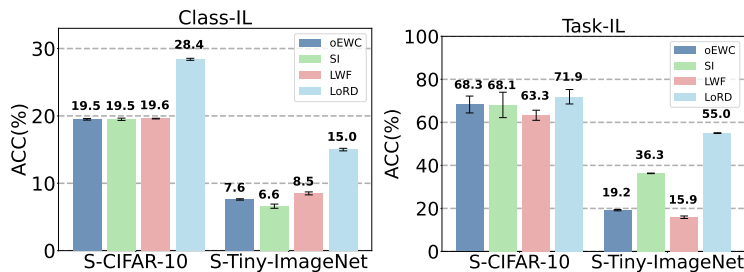


Figure 3: Classification results for standard buffer-free CL benchmarks.

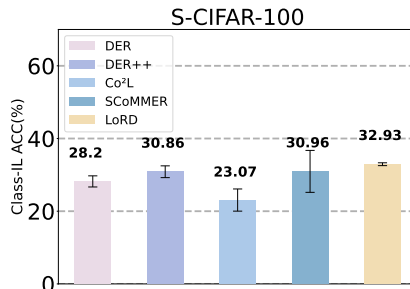


Figure 4: Results of different methods on S-CIFAR-100 with an unknown number of tasks and a buffer size of 500.

effectively mitigates *catastrophic forgetting* and optimizes performance without prior knowledge of the task count.

*Forgetting Analysis.* Tab. 3 presents the FF result. Our method demonstrates the lowest level of forgetting, highlighting its effectiveness in preserving previously acquired knowledge. This indicates that LoRD not only improves the performance of subsequent tasks but also mitigates the challenge of *catastrophic forgetting*, emphasizing the importance of decoupling task-specific knowledge to maintain stability across tasks.

*Results with Different Task Settings.* To evaluate the capacity of various methods for knowledge assimilation, we compared our method against other methods using the S-CIFAR-100 dataset, covering different task settings. Specifically, we evaluate performances in settings of 5, 10, and 20 tasks. Tab. 4 presents the performance evaluation of our method on the S-CIFAR-100 dataset. Across all task settings, our method con-

Table 3: Forgetting results on S-CIFAR-10 dataset.

Method	S-CIFAR-10			
	Class-IL(↓)		Task-IL(↓)	
LoRD w/o BUF	28.37		71.85	
Buffer Size	200	500	200	500
GEM	82.61±1.60	74.31±4.62	9.27±2.07	9.12±0.21
iCaRL	28.72±0.49	25.71±1.10	<b>2.63±3.48</b>	2.66±2.47
ER	61.24±2.62	74.35±0.07	7.08±0.64	3.54±0.35
A-GEM	95.73±0.20	94.01±1.16	16.39±0.86	14.26±4.18
GSS	75.25±4.07	62.88±2.67	8.56±1.78	7.73±3.99
DER	40.76±0.42	26.74±0.15	6.57±0.20	4.56±0.45
DER++	32.59±4.41	22.38±0.84	5.16±1.15	4.66±0.19
HAL	69.11±4.34	62.21±7.53	12.26±1.10	5.41±0.50
ER-ACE	35.79±5.77	24.51±1.80	6.92±0.66	4.07±0.28
SCoMMER	23.73±4.76	16.85±1.35	6.92±1.16	2.86±0.47
<b>LoRD (ours)</b>	<b>23.54±3.22</b>	<b>16.68±2.15</b>	<b>4.19±0.20</b>	<b>1.84±0.31</b>

sistently outperforms other existing methods. In Class-IL, our LoRD achieves a 2.06% and 2% ACC improvement over the sub-optimal method SCoMMER on the S-CIFAR-100 dataset with 10 and 20 tasks, which is quite notable. This result highlights that LoRD not only excels at integrating short-term knowledge but also effectively assimilates long-term knowledge, thereby significantly alleviating forgetting. This strongly corroborates LoRD’s robustness across multiple task settings and showcases its remarkable generalization ability.

#### 4.6. Ablation Study

Tab. 5 shows the ablation studies for each component in LoRD on S-CIFAR-10 datasets. To assess the influence of the replay buffer, we conduct an experimental evaluation by removing the replay buffer component from the LoRD model (LoRD

Table 4: Comparison of different methods for S-CIFAR-100 dataset with a buffer size of 500.  $\mathcal{T}$  denotes the number of tasks.

Method	S-CIFAR-100					
	Class-IL( $\uparrow$ )			Task-IL( $\uparrow$ )		
Number of Tasks	$\mathcal{T} = 20$	$\mathcal{T} = 10$	$\mathcal{T} = 5$	$\mathcal{T} = 20$	$\mathcal{T} = 10$	$\mathcal{T} = 5$
DER	28.20 $\pm$ 1.53	33.25 $\pm$ 2.72	40.17 $\pm$ 2.26	78.19 $\pm$ 0.16	74.62 $\pm$ 0.65	70.25 $\pm$ 0.07
DER++	30.86 $\pm$ 1.62	36.68 $\pm$ 1.25	42.34 $\pm$ 2.82	79.54 $\pm$ 0.78	75.49 $\pm$ 0.36	70.81 $\pm$ 0.19
$Co^2L$	23.07 $\pm$ 3.05	27.51 $\pm$ 1.04	29.42 $\pm$ 4.46	61.46 $\pm$ 5.81	54.85 $\pm$ 3.37	49.09 $\pm$ 6.19
SCOMMER	30.96 $\pm$ 5.77	38.55 $\pm$ 5.77	47.27 $\pm$ 5.77	84.12 $\pm$ 5.77	80.08 $\pm$ 5.77	74.75 $\pm$ 5.77
<b>LoRD (Ours)</b>	<b>32.93<math>\pm</math>0.39</b>	<b>40.61<math>\pm</math>1.24</b>	<b>48.11<math>\pm</math>0.80</b>	80.15 $\pm$ 0.30	76.44 $\pm$ 0.43	73.18 $\pm$ 0.41

Table 5: Ablation studies of LoRD with 200 buffer size on S-CIFAR-10 dataset.

Method	S-CIFAR-10			
	Class-IL( $\uparrow$ )	Task-IL( $\uparrow$ )	Forgetting( $\downarrow$ )	FLOPs Train $\times 10^{15}$ ( $\downarrow$ )
LoRD <i>w/o</i> BUF	28.37 $\pm$ 4.63	71.85 $\pm$ 5.80	90.78 $\pm$ 1.64	6.28
LoRD <i>w/o</i> $\mathcal{L}_{PD}$	64.37 $\pm$ 1.37	92.32 $\pm$ 0.62	34.76 $\pm$ 3.42	8.71
LoRD <i>w/o</i> $\mathcal{L}_{DER}$	67.45 $\pm$ 2.36	92.42 $\pm$ 0.29	25.11 $\pm$ 0.441	8.03
LoRD <i>w/o</i> Compression	65.04 $\pm$ 4.90	91.39 $\pm$ 1.63	26.67 $\pm$ 4.90	16.67
LoRD <i>w/o</i> Pruning	68.16 $\pm$ 1.44	93.39 $\pm$ 0.29	22.61 $\pm$ 12.21	9.90
LoRD <i>w/o</i> TRS	68.97 $\pm$ 2.74	93.47 $\pm$ 0.14	29.79 $\pm$ 5.07	9.77
<b>LoRD</b>	<b>70.16<math>\pm</math>0.36</b>	<b>93.94<math>\pm</math>0.36</b>	23.54 $\pm$ 3.22	9.77

*w/o* BUF). LoRD *w/o* Compression means that the learnable parameters of the student model are not compressed across tasks, while LoRD *w/o* Pruning means that the teacher model is not pruned. From the results, we have the following observations: (1) The results of LoRD *w/o*  $\mathcal{L}_{PD}$  and LoRD *w/o*  $\mathcal{L}_{DER}$  indicate that the collaborative use of both distillation losses is crucial for the teacher network to efficiently encode useful knowl-

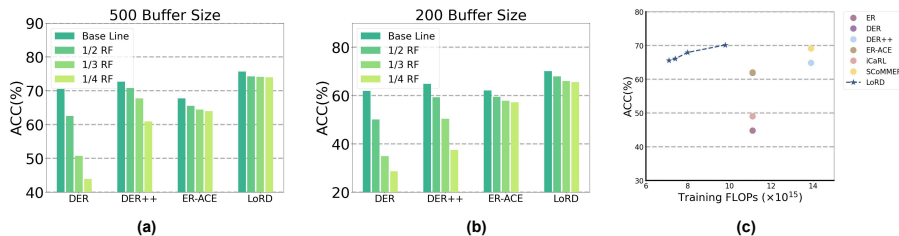


Figure 5: Results for the quantitative analysis. (a) and (b) illustrate the accuracy at varying rehearsal frequencies. (c) displays the training FLOPs and accuracy of different methods.

edge.  $\mathcal{L}_{PD}$  aims to maintain the integrity of past knowledge by continuously updating the teacher network.  $\mathcal{L}_{DER}$ , on the other hand, focuses on preventing forgetting in both the student and teacher networks, thereby enabling more effective encoding of valuable knowledge. The synergistic effect of these two distillation losses can significantly enhance the effectiveness of model distillation. (2) The results of LoRD *w/o* Compression and LoRD *w/o* Pruning indicate that eliminating redundancy during the distillation process is crucial for achieving a balance between model plasticity and stability, and is also essential for boosting training efficiency. (3) TRS has been proven to be positive in efficiently selecting saved samples, improving storage utilization, and achieving higher ACC under limited buffer sizes. (4) LoRD attains superior ACC by comprehensively deploying all components, thus corroborating the efficacy of its components.<sup>2</sup>

#### 4.7. Quantitative Study

In this section, we present a comprehensive analysis of our method LoRD by conducting a comparative study against existing SOTA CL methods.

*Rehearsal Frequency.* Due to the use of the teacher model, it has become unnecessary to replay in every batch. In our experiment, we decrease the RF to reduce the high computational complexity in rehearsal methods and enhance training efficiency. Fig. 5 (a) and (b) showcase the ACC of different methods across various RF on the S-CIFAR-10 dataset. When reducing RF, LoRD exhibits a considerably smaller impact than other

<sup>2</sup>We provide more extensive ablation studies about each component in Appendix D.

Table 6: Comparison of LoRD and various methods using SparCL on S-CIFAR-10 dataset (Sparsity Ratio: 0.75, Buffer Size: 200).

Method	S-CIFAR-10		
	Class-IL( $\uparrow$ )	Task-IL( $\uparrow$ )	FLOPs Train $\times 10^{15}$ ( $\downarrow$ )
ER-SparCL	46.89 $\pm$ 0.68	92.02 $\pm$ 0.72	2.0
DER++-SparCL	66.30 $\pm$ 0.98	<b>94.06<math>\pm</math>0.45</b>	2.5
<b>LoRD-SparCL</b>	<b>67.07<math>\pm</math>1.65</b>	93.98 $\pm$ 0.15	<b>1.7</b>

Table 7: Comparison of training FLOPs across different methods on multiple benchmark datasets.

Method	S-CIFAR-10	S-CIFAR-100	S-Tiny-ImageNet
ER	$11.1 \times 10^{15}$	$11.1 \times 10^{15}$	$17.8 \times 10^{16}$
DER++	$13.9 \times 10^{15}$	$13.9 \times 10^{15}$	$22.2 \times 10^{16}$
ER-ACE	$11.1 \times 10^{15}$	$11.1 \times 10^{15}$	$17.8 \times 10^{16}$
SCoMMER	$13.9 \times 10^{15}$	$13.9 \times 10^{15}$	$22.2 \times 10^{16}$
<b>LoRD</b>	$9.8 \times 10^{15}$	$4.6 \times 10^{15}$	$12.0 \times 10^{16}$

methods. At a buffer size of 500 and 200, with the RF adjusted to 1/4, LoRD demonstrates only a 1.68% and 4.58% decrease in ACC, respectively. Additionally, ER-ACE outperforms DER++ and DER due to its cross-entropy computation based solely on the current task’s classes, which enhances model stability and reduces reliance on replay samples. Consequently, LoRD can dynamically adjust the RF to balance accuracy and efficiency, making it adaptable to various scenarios, including edge computing, with minimal accuracy degradation.

*Training Efficiency.* Minimizing overall training FLOPs is crucial when dealing with data streams to ensure that training keeps pace with the rate at which data becomes available [39]. Studies [9] have shown that in real-world applications, the ER method performs best due to its high training efficiency. Therefore, when designing CL meth-

Table 8: Comparison of different methods for the S-CIFAR-10 dataset using Nvidia Jetson TX2 with a buffer size of 200 in an online CL setting.

Method	S-CIFAR-10	
	Class-IL( $\uparrow$ )	
Buffer Size	200	500
ER	37.64 $\pm$ 15.46	45.22 $\pm$ 9.49
DER++	41.93 $\pm$ 11.94	48.04 $\pm$ 6.39
ER-ACE	41.18 $\pm$ 10.79	44.30 $\pm$ 4.79
SCoMMER	18.20 $\pm$ 0.94	20.92 $\pm$ 0.89
<b>LoRD</b>	<b>44.92<math>\pm</math>9.30</b>	<b>48.41<math>\pm</math>5.76</b>

ods, it is important to ensure that training FLOPs do not exceed those of ER. For comprehensive evaluation, we quantify the cumulative training FLOPs upon completion of terminal tasks across comparative methods. As presented in Tab. 7, our proposed LoRD consistently achieves the minimal training FLOPs across all benchmark datasets, with particularly pronounced efficiency gains in large-scale task configurations (e.g., 20-task S-CIFAR-100). This enhanced scalability stems from our cosine-annealed model compression mechanism (see Eq. (5)), where a higher N value enables the model to maintain elevated compression ratios throughout extended task sequences, thereby achieving FLOPs reduction in prolonged continual learning scenarios. Complementary analysis in Fig. 5 (c) on S-CIFAR-10 (buffer size=200) reveals that LoRD achieves the highest ACC with the lowest training FLOPs, occupying the optimal upper-left position in the performance-efficiency landscape. This observation confirms that our compression strategy improves training efficiency without compromising accuracy. Furthermore, by modulating the RF, LoRD facilitates a flexible balance between computational efficiency and predictive accuracy, rendering it adaptable to diverse application requirements across resource-constrained and precision-sensitive environments.

*Sparse Training.* To evaluate the compatibility of LoRD with other efficient CL methods, we train our model using the SOTA sparse training method SparCL [11] and test training FLOPs and ACC. We employ a dynamic masking mechanism to selectively mask the weights of the student model. Concurrently, in the weight update phase, a dynamic gradient masking mechanism is utilized to selectively update specific weights during backpropagation. After a certain number of training epochs, data samples that have been well-learned by the model are filtered out, allowing the method to focus more on samples with higher classification difficulty. To address the overfitting issue, we alternate between the distillation method and replay samples in each training batch. Tab. 6 demonstrates the results of integrating LoRD with SparCL. In contrast to the suboptimal DER++ method, LoRD boosts ACC by 0.77% and slashes training FLOPs by 32%. The outstanding performance of LoRD highlights its effectiveness in eliminating network redundancy. Moreover, the successful integration of LoRD and SparCL demonstrates LoRD’s adaptability to sparse training, indicating its potential compatibility with pruning methods.

*Online CL on Real Edge Devices.* We conduct single-epoch training on real edge devices to simulate real-world online CL scenarios [40]. Tab. 8 presents the ACC of different methods under the online CL setting on Nvidia Jetson TX2. LoRD achieves the highest ACC across various buffer sizes. This not only validates its reliability in complex real-world scenarios but also highlights its exceptional scalability and efficiency in resource-constrained edge computing and low-resource environments, indicating its highly promising practical applicability.

## 5. Conclusion

To reduce redundancy in the continual learning process, we draw inspiration from the brain’s contextual gating mechanism and propose Low-redundancy Distillation. LoRD aims to enhance model performance while maintaining training efficiency through collaborative optimization. LoRD involves pruning the teacher model and compressing the student model’s learnable parameters to facilitate the retention and optimization of prior knowledge, effectively decoupling task-specific knowledge without the need to

manually assign isolated parameters for each task. Furthermore, we optimize the selection of rehearsal samples and refine RF to improve training efficiency. Extensive experimentation across various benchmark datasets and environments demonstrates LoRD’s superiority, achieving the highest accuracy within the same training time and requiring the minimum training FLOPs to achieve comparable accuracy.

LoRD is subject to three primary limitations. Firstly, in the context of long task sequences, the student model’s compression strategy applies a higher compression rate to earlier tasks, which, while yielding significant computational benefits, compromises the performance of these initial models. This reflects an inherent trade-off between accuracy and efficiency, necessitating careful consideration of compression parameters to balance these objectives. Secondly, a key limitation of LoRD is its dependence on predefined task boundaries, an assumption that may not hold in dynamic real-world environments where tasks lack clear delineation. This reliance on prior knowledge of task transitions constrains the method’s adaptability, potentially impairing performance in scenarios with unstable or overlapping task structures. Thirdly, LoRD is currently tailored exclusively to visual models and specific network architectures, limiting its applicability across diverse domains and model types. Furthermore, LoRD may exhibit an increased memory footprint when processing large-scale datasets.

To address these limitations, future work can pursue targeted enhancements. For the first limitation, developing adaptive compression strategies that dynamically adjust the compression rate—based on task importance or real-time performance metrics—could preserve early task performance while retaining computational gains. For the second limitation, exploring methods to reduce dependency on predefined task boundaries, such as unsupervised techniques for detecting task shifts, could enhance LoRD’s flexibility in real-world settings with fluid task structures. For the third limitation, extending LoRD’s applicability to additional domains, such as natural language processing or reinforcement learning, and adapting it to diverse architectures, including recurrent or transformer-based models, would broaden its utility and generalizability across a wider range of continual learning scenarios.

## Appendix A Teacher-aware Reservoir Sampling

### A.1 Sample preservation probability in the TRS method

Here we will use mathematical induction to calculate the probability of retaining the sample in the buffer. For the first  $\mathcal{B}$  samples  $x_1, x_2, \dots, x_{\mathcal{B}}$ , we will keep them in the buffer, and  $p(x_1 \text{ is retained}) = p(x_2 \text{ is retained}) = \dots = p(x_{\mathcal{B}} \text{ is retained}) = 1$ . For the  $k$ -th ( $k > \mathcal{B}$ ) sample, we keep it with a probability of  $p(x_k) = \exp(-\alpha \frac{|\psi_{t1}|}{|\theta_{t1}|}) \frac{\mathcal{B}}{k}$  (which only means it is retained this time). So the probability of being retained in the first  $\mathcal{B}$  samples  $x_r (r \in 1 : \mathcal{B})$  can be expressed as follows:

$$\begin{aligned} p(x_r \text{ is retained}) = \\ p(x_r \text{ was retained in the previous round}) \times \\ (p(x_k \text{ is discarded}) + p(x_k \text{ is retained}) \times p(x_r \text{ not replaced})) \end{aligned}$$

**Theorem 1.** For any positive integer  $k (\mathcal{B} < k)$ , the following equation holds:

$$p(x_r) = \prod_{n=\mathcal{B}+1}^k \frac{\exp(\alpha \frac{|\psi_{t1}|}{|\theta_{t1}|}) - 1}{\exp(\alpha \frac{|\psi_{t1}|}{|\theta_{t1}|})}$$

We will prove this equation using mathematical induction.

**Base Step:** When  $k = \mathcal{B}+1$ , the sum on the left-hand side is  $1 \times ((1 - \exp(-\alpha \frac{|\psi_{t1}|}{|\theta_{t1}|}) \frac{\mathcal{B}}{\mathcal{B}+1})) + \exp(-\alpha \frac{|\psi_{t1}|}{|\theta_{t1}|}) \frac{\mathcal{B}}{\mathcal{B}+1} \times \frac{\mathcal{B}-1}{\mathcal{B}} = \frac{(\mathcal{B}+1)\exp(\alpha \frac{|\psi_{t1}|}{|\theta_{t1}|}) - 1}{(\mathcal{B}+1)\exp(\alpha \frac{|\psi_{t1}|}{|\theta_{t1}|})}$ , and the right-hand side evaluates to  $\frac{(\mathcal{B}+1)\exp(\alpha \frac{|\psi_{t1}|}{|\theta_{t1}|}) - 1}{(\mathcal{B}+1)\exp(\alpha \frac{|\psi_{t1}|}{|\theta_{t1}|})}$  as well. Therefore, the equation holds.

**Inductive Hypothesis:** Assume that the equation holds for  $k = m$ , i.e.,  $p(x_r) = \prod_{n=\mathcal{B}+1}^m \frac{\exp(\alpha \frac{|\psi_{t1}|}{|\theta_{t1}|}) - 1}{\exp(\alpha \frac{|\psi_{t1}|}{|\theta_{t1}|})}$ .

**Inductive Step:** We need to show that the equation also holds for  $k = m + 1$ . We can expand the sum on the left-hand side as:

$$\begin{aligned} p(x_r) = p(x_r \text{ was retained in the previous round}) \times \\ ((1 - \exp(-\alpha \frac{|\psi_{t1}|}{|\theta_{t1}|}) \frac{\mathcal{B}}{m+1})) + \\ \exp(-\alpha \frac{|\psi_{t1}|}{|\theta_{t1}|}) \frac{\mathcal{B}}{m+1} \times \frac{\mathcal{B}-1}{\mathcal{B}} \end{aligned}$$

Using the inductive hypothesis,  $p(x_r \text{ was retained in the previous round})$  is equal to

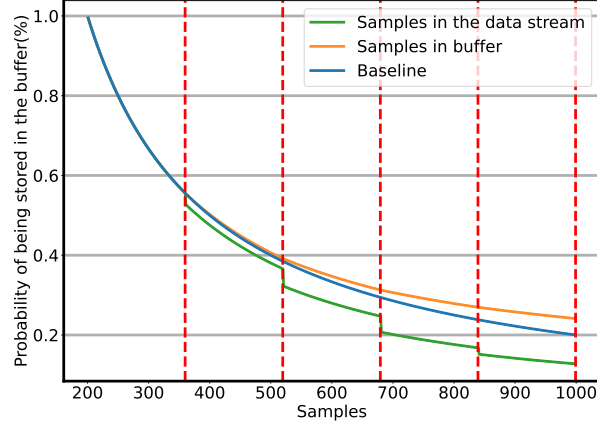


Figure A.6: The probability of different data being stored in the buffer, where the **blue** line represents the reserve sampling method, which ensures an equal probability of storage in the buffer for all data.

$\prod_{n=\mathcal{B}+1}^m \frac{\text{nexp}(\alpha \frac{|\psi_r|}{|\theta_r|}) - 1}{\text{nexp}(\alpha \frac{|\psi_r|}{|\theta_r|})}$ . Thus, we can rewrite the above expression as:

$$\prod_{n=\mathcal{B}+1}^{m+1} \frac{\text{nexp}(\alpha \frac{|\psi_r|}{|\theta_r|}) - 1}{\text{nexp}(\alpha \frac{|\psi_r|}{|\theta_r|})}$$

Simplifying, we get:

$$p(x_r) = \prod_{n=\mathcal{B}+1}^{m+1} \frac{\text{nexp}(\alpha \frac{|\psi_r|}{|\theta_r|}) - 1}{\text{nexp}(\alpha \frac{|\psi_r|}{|\theta_r|})}$$

This proves that the equation holds for  $k = m + 1$ .

By the principle of mathematical induction, the equation holds for any positive integer  $n$ .

Fig. A.6 illustrates the probability of storing individual samples in a buffer under the TRS method, with the parameters  $|\mathcal{D}| = 1000$  and  $\mathcal{B} = 200$ .

## Appendix B Hyperparameter Selection

Tab. B.9 presents the selected optimal hyperparameter combinations for each method in the main paper. The hyperparameters include the learning rate (lr), batch size (bs), and minibatch size (mbs) for rehearsal-based methods. Other symbols correspond to specific methods. It should be noted that the batch size and minibatch size are held constant at 32 for all CL benchmarks.

Table B.9: Hyperparameters selected for our experiments.

Method	Buffer	Split Tiny ImageNet	Buffer	Split CIFAR-10
SGD	-	$lr: 0.03$	-	$lr: 0.1$
oEWC	-	$lr: 0.03 \ \lambda: 90 \ \gamma: 1.0$	-	$lr: 0.03 \ \lambda: 10 \ \gamma: 1.0$
SI	-	$lr: 0.03 \ c: 1.0 \ \xi: 0.9$	-	$lr: 0.03 \ c: 0.5 \ \xi: 1.0$
LwF	-	$lr: 0.01 \ \alpha: 1 \ T: 2.0$	-	$lr: 0.03 \ \alpha: 0.5 \ T: 2.0$
ER	200	$lr: 0.1$	200	$lr: 0.1$
	500	$lr: 0.03$	500	$lr: 0.1$
GEM			200	$lr: 0.03 \ \gamma: 0.5$
			500	$lr: 0.03 \ \gamma: 0.5$
A-GEM	200	$lr: 0.01$	200	$lr: 0.03$
	500	$lr: 0.01$	500	$lr: 0.03$
iCaRL	200	$lr: 0.03 \ wd: 10^{-5}$	200	$lr: 0.1 \ wd: 10^{-5}$
	500	$lr: 0.03 \ wd: 10^{-5}$	500	$lr: 0.1 \ wd: 10^{-5}$
GSS			200	$lr: 0.03 \ gmb: 32 \ nb: 1$
			500	$lr: 0.03 \ gmb: 32 \ nb: 1$
HAL			200	$lr: 0.03 \ \lambda: 0.2 \ \beta: 0.5$
				$\gamma: 0.1$
			500	$lr: 0.03 \ \lambda: 0.1 \ \beta: 0.3$
				$\gamma: 0.1$
DER	200	$lr: 0.03 \ \alpha: 0.1$	200	$lr: 0.03 \ \alpha: 0.3$
	500	$lr: 0.03 \ \alpha: 0.1$	500	$lr: 0.03 \ \alpha: 0.3$
DER++	200	$lr: 0.03 \ \alpha: 0.1 \ \beta: 1.0$	200	$lr: 0.03 \ \alpha: 0.1 \ \beta: 0.5$
	500	$lr: 0.03 \ \alpha: 0.2 \ \beta: 0.5$	500	$lr: 0.03 \ \alpha: 0.2 \ \beta: 0.5$
Co <sup>2</sup> L	200	$lr: 0.03 \ \kappa: 0.1 \ \kappa^*: 0.1$	200	$lr: 0.03 \ \kappa: 0.2 \ \kappa^*: 0.01$
		$\eta: 0.1 \ \tau: 0.5$		$\eta: 0.5 \ \tau: 0.5$
	500	$lr: 0.03 \ \kappa: 0.1 \ \kappa^*: 0.1$	500	$lr: 0.03 \ \kappa: 0.2 \ \kappa^*: 0.01$
		$\eta: 0.1 \ \tau: 0.5$		$\eta: 0.5 \ \tau: 0.5$
ER-ACE	200	$lr: 0.1$	200	$lr: 0.1$
	500	$lr: 0.1$	500	$lr: 0.1$
SCoMMER	200	$lr: 0.1 \ \pi_h: 0.5 \ \pi_s: 2$	200	$lr: 0.1 \ \pi_h: 0.5 \ \pi_s: 2$
		$r: 0.1$		$r: 0.5$
	500	$lr: 0.1 \ \pi_h: 0.5 \ \pi_s: 2$	500	$lr: 0.1 \ \pi_h: 0.5 \ \pi_s: 2$
		$r: 0.15$		$r: 0.7$
LoRD	200	$lr: 0.1 \ \beta_1: 1.0 \ \beta_2: 0.1$	200	$lr: 0.1 \ \beta_1: 0.5 \ \beta_2: 0.1$
		$G: 19 \ \alpha: 0.75 \ \lambda: 0.05$		$G: 10 \ \alpha: 0.75 \ \lambda: 0.05$
	500	$lr: 0.1 \ \beta_1: 0.5 \ \beta_2: 0.2$	500	$lr: 0.1 \ \beta_1: 0.5 \ \beta_2: 0.2$
		$G: 19 \ \alpha: 0.75 \ \lambda: 0.05$		$G: 10 \ \alpha: 0.75 \ \lambda: 0.05$

Method	Buffer	Split CIFAR-100
DER	500	$lr: 0.03 \ \alpha: 0.1$
DER++	500	$lr: 0.03 \ \alpha: 0.2 \ \beta: 0.5$
Co <sup>2</sup> L	500	$lr: 0.03 \ \kappa: 0.2 \ \kappa^*: 0.01$
		$\eta: 0.5 \ \tau: 0.5$
SCoMMER	500	$lr: 0.1 \ \pi_h: 0.5 \ \pi_s: 2$
		$r: 0.1$
LoRD	500	$lr: 0.1 \ \beta_1: 1.0 \ \beta_2: 0.1$
		$G: 19 \ \alpha: 0.75 \ \lambda: 0.05$

## Appendix C Hyperparameter Sensitivity

In Tab. C.10, we report the performance of LoRD against a range of hyperparameters.  $\alpha$  (Eq. 10 in the main paper) controls the subsequent impact of teacher subnet size on TRS. A larger value of  $\alpha$  results in fewer samples being retained for new tasks.  $\lambda$  (Eq. 11 in the main paper) controls the distillation effect of the teacher subnet on model training. A larger  $\lambda$  value reduces the likelihood of the student model forgetting previous tasks, but it also makes learning new tasks more challenging. Experimental results indicate that optimal performance of LoRD is achieved when parameters  $\alpha$  and  $\lambda$  are set to 0.75 and 0.05, respectively. More importantly, LoRD exhibits low sensitivity to

Table C.10: Average Accuracy of LoRD on different values of hyperparameters. For a given hyperparameter in the table, all the other hyperparameters are set to their optimal values.

Method	S-CIFAR-10			
	Class-IL( $\uparrow$ )		Task-IL( $\uparrow$ )	
Buffer Size	200	500	200	500
$\alpha = 0.125$	68.16	74.92	93.41	94.74
$\alpha = 0.25$	68.53	74.46	93.33	94.41
$\alpha = 0.375$	69.44	75.04	93.64	94.54
$\alpha = 0.5$	69.33	75.68	93.65	94.81
$\alpha = 0.625$	68.97	75.66	93.66	94.97
$\alpha = 0.75$	70.04	75.10	93.94	94.90
$\alpha = 0.875$	70.06	74.95	93.71	94.93
$\alpha = 1$	69.22	74.90	93.84	94.79
$\lambda = 0.01$	68.18	75.16	93.60	94.59
$\lambda = 0.025$	69.35	74.97	93.71	94.78
$\lambda = 0.05$	70.16	75.66	93.75	94.95
$\lambda = 0.075$	68.93	75.46	93.60	94.88
$\lambda = 0.2$	68.85	74.93	93.71	94.83
$\lambda = 0.5$	68.90	74.85	93.88	94.39

Table C.11: Comparison of Different Expansion Methods on S-CIFAR-10 dataset.

Method	S-CIFAR-10	
	Class-IL( $\uparrow$ )	Task-IL( $\uparrow$ )
LoRD <i>w/o</i> Compression	20.16	71.15
LoRD <i>w/</i> Linear	25.62	68.08
<b>LoRD <i>w/</i> Cos</b>	<b>28.37</b>	<b>71.85</b>

hyperparameter selection, significantly enhancing its user-friendliness.

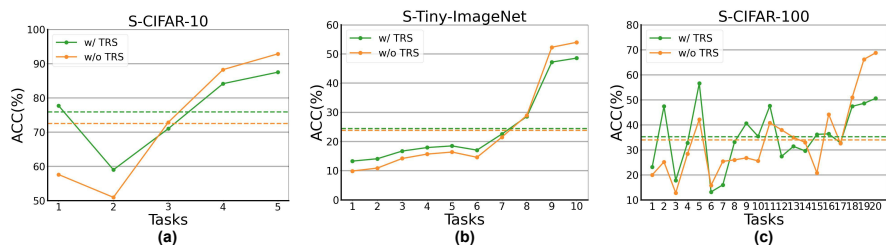


Figure D.7: Classification performance across datasets in ablation experiments.

## Appendix D Ablation Study

### D.1 Student Model Compression

We study the impact of different parameter allocation methods on model performance without buffer. Tab. C.11 presents the results obtained by allowing all parameters to update (LoRD *w/o* Compression), linearly allocating parameters (LoRD *w/* Linear), and cosine allocating parameters (LoRD *w/* Cos). The results indicate that utilizing cosine parameter allocation greatly enhances the LoRD’s performance. Not restricting parameter updates from the beginning can cause the student model to quickly reach saturation, while linearly allocating parameters may constrain the student model’s initial performance. Both scenarios can lead to a decline in the model’s overall performance. These experiments provide valuable insights into the significance of student model compression.

### D.2 Teacher model Pruning

When the teacher model is not pruned, we directly use the student model from the last task as the teacher model for the current task. However, this method does not consider the varying additional parameters required by different tasks. Similar tasks often require fewer additional parameters, indicating a higher degree of similarity between the teacher subnet. On the other hand, tasks with significant differences require more additional parameters, representing larger teacher subnet differences. By pruning the teacher model, LoRD can automatically identify the similarity between tasks to improve performance.

### D.3 Teacher-aware Reservoir Sampling

As depicted in Fig. D.7, the experimental results showcase the task-specific classification accuracy of the proposed method across various datasets. The integration of the TRS module enables LoRD to attain a more balanced and representative learning of prior knowledge, thereby resulting in a substantial enhancement in performance.

### D.4 Different loss function selection

Our method uses two distillation losses  $\mathcal{L}_{PD}$  and  $\mathcal{L}_{DER++}$ , where  $\mathcal{L}_{CE}$  is on all tasks' logits. We conduct additional experiments to verify the efficacy of LoRD in decoupling task-specific knowledge. First, we calculate  $\mathcal{L}_{CE}$  solely on the classes of the current task, denoted as  $\mathcal{L}_{ACE}$ . Then, we decompose  $\mathcal{L}_{DER++}$  into two components: one that only calculates cross-entropy on samples from previous tasks, denoted as  $\mathcal{L}_{ER}$ , and another that aligns the logits of samples from previous tasks, denoted as  $\mathcal{L}_{DER}$ . As shown in Tab. D.12, our method yields the highest accuracy by low-redundancy distillation, which restricts the learning capabilities of the distilled subnets for new tasks. Consequently, only the non-distilled subnets can rapidly adapt to new tasks, effectively addressing the task recency bias problem. Meanwhile, the poor performance observed in  $\mathcal{L}_{ACE}$  further substantiates our viewpoint. This is because LoRD effectively decouples task-specific knowledge, while calculating the cross-entropy only on the current task's classes would severely impair model's learning on the present task.

Table D.12: Effect of different loss functions with a buffer size of 200.

Loss Function	$\mathcal{L}_{ACE}$	$\mathcal{L}_{ER}$	$\mathcal{L}_{DER}$	$\mathcal{L}_{DER++}$
<b>S-CIFAR-10 Acc</b>	55.82	67.45	68.25	70.16

## References

- [1] Da-Wei Zhou, Qi-Wei Wang, Zhi-Hong Qi, Han-Jia Ye, De-Chuan Zhan, and Ziwei Liu. Class-incremental learning: A survey. *IEEE Transactions on Pattern Analysis and Machine Intelligence*, 2024.

- [2] Michael McCloskey and Neal J Cohen. Catastrophic interference in connectionist networks: The sequential learning problem. In *Psychology of learning and motivation*, volume 24, pages 109–165. Elsevier, 1989.
- [3] Rui Yang, Shuang Wang, Yu Gu, Jihui Wang, Yingzhi Sun, Huan Zhang, Yu Liao, and Licheng Jiao. Continual learning for cross-modal image-text retrieval based on domain-selective attention. *Pattern Recognition*, 149:110273, 2024.
- [4] Hangda Liu, Boyu Diao, Wenxin Chen, and Yongjun Xu. A resource-aware workload scheduling method for unbalanced gemms on gpus. *The Computer Journal*, page bxae110, 2024.
- [5] Mustafa B Gurbuz and Constantine Dovrolis. Nispa: Neuro-inspired stability-plasticity adaptation for continual learning in sparse networks. In *Proceedings of the 39th International Conference on Machine Learning*, volume 162, 2022.
- [6] Lu Yu, Bartłomiej Twardowski, Xialei Liu, Luis Herranz, Kai Wang, Yongmei Cheng, Shangling Jui, and Joost van de Weijer. Semantic drift compensation for class-incremental learning. In *Proceedings of the IEEE/CVF conference on computer vision and pattern recognition*, pages 6982–6991, 2020.
- [7] Pietro Buzzega, Matteo Boschini, Angelo Porrello, Davide Abati, and Simone Calderara. Dark experience for general continual learning: a strong, simple baseline. *Advances in neural information processing systems*, 33:15920–15930, 2020.
- [8] Anthony Robins. Catastrophic forgetting, rehearsal and pseudorehearsal. *Connection Science*, 7(2):123–146, 1995.
- [9] Ameya Prabhu, Hasan Abed Al Kader Hammoud, Puneet K Dokania, Philip HS Torr, Ser-Nam Lim, Bernard Ghanem, and Adel Bibi. Computationally budgeted continual learning: What does matter? In *Proceedings of the IEEE/CVF Conference on Computer Vision and Pattern Recognition*, pages 3698–3707, 2023.
- [10] Ruiqi Liu, Boyu Diao, Libo Huang, Zijia An, Zhulin An, and Yongjun Xu. Continual learning in the frequency domain. *arXiv preprint arXiv:2410.06645*, 2024.

- [11] Zifeng Wang, Zheng Zhan, Yifan Gong, Geng Yuan, Wei Niu, Tong Jian, Bin Ren, Stratis Ioannidis, Yanzhi Wang, and Jennifer Dy. Sparcl: Sparse continual learning on the edge. *Advances in Neural Information Processing Systems*, 35:20366–20380, 2022.
- [12] Xiaorong Li, Shipeng Wang, Jian Sun, and Zongben Xu. Memory efficient data-free distillation for continual learning. *Pattern Recognition*, 144:109875, 2023.
- [13] Matteo Boschini, Lorenzo Bonicelli, Pietro Buzzega, Angelo Porrello, and Simone Calderara. Class-incremental continual learning into the extended der-verse. *IEEE transactions on pattern analysis and machine intelligence*, 45(5):5497–5512, 2022.
- [14] Lucas Caccia, Rahaf Aljundi, Nader Asadi, Tinne Tuytelaars, Joelle Pineau, and Eugene Belilovsky. New insights on reducing abrupt representation change in online continual learning. In *International Conference on Learning Representations*, 2022.
- [15] Yasir Ghunaim, Adel Bibi, Kumail Alhamoud, Motasem Alfarra, Hasan Abed Al Kader Hammoud, Ameya Prabhu, Philip HS Torr, and Bernard Ghanem. Real-time evaluation in online continual learning: A new hope. In *Proceedings of the IEEE/CVF conference on computer vision and pattern recognition*, pages 11888–11897, 2023.
- [16] Dhireesha Kudithipudi, Mario Aguilar-Simon, Jonathan Babb, Maxim Bazhenov, Douglas Blackiston, Josh Bongard, Andrew P Brna, Suraj Chakravarthi Raja, Nick Cheney, Jeff Clune, et al. Biological underpinnings for lifelong learning machines. *Nature Machine Intelligence*, 4(3):196–210, 2022.
- [17] Zhizhong Li and Derek Hoiem. Learning without forgetting. *IEEE transactions on pattern analysis and machine intelligence*, 40(12):2935–2947, 2017.
- [18] Libo Huang, Yan Zeng, Chuanguang Yang, Zhulin An, Boyu Diao, and Yongjun Xu. etag: Class-incremental learning via embedding distillation and task-oriented

- generation. In *Proceedings of the AAAI Conference on Artificial Intelligence*, volume 38, pages 12591–12599, 2024.
- [19] Wenju Sun, Qingyong Li, Jing Zhang, Danyu Wang, Wen Wang, and YangLi-ao Geng. Exemplar-free class incremental learning via discriminative and comparable parallel one-class classifiers. *Pattern Recognition*, 140:109561, 2023.
- [20] David Lopez-Paz and Marc’ Aurelio Ranzato. Gradient episodic memory for continual learning. *Advances in neural information processing systems*, 30, 2017.
- [21] Zhizheng Wang, Yuanyuan Sun, Xiaokun Zhang, Bo Xu, Zhihao Yang, and Hongfei Lin. Continual learning with high-order experience replay for dynamic network embedding. *Pattern Recognition*, 159:111093, 2025.
- [22] Md Y Harun, J Gallardo, Tyler L Hayes, Ronald Kemker, and Christopher Kanan. Siesta: Efficient online continual learning with sleep. *Transactions on Machine Learning Research*, 2023.
- [23] Geoffrey Hinton, Oriol Vinyals, and Jeff Dean. Distilling the knowledge in a neural network. *arXiv preprint arXiv:1503.02531*, 2015.
- [24] Han Cai, Chuang Gan, Tianzhe Wang, Zhekai Zhang, and Song Han. Once for all: Train one network and specialize it for efficient deployment. In *International Conference on Learning Representations*, 2020.
- [25] Esteban Real, Alok Aggarwal, Yanping Huang, and Quoc V Le. Regularized evolution for image classifier architecture search. In *Proceedings of the aaai conference on artificial intelligence*, volume 33, pages 4780–4789, 2019.
- [26] Jaehong Yoon, Divyam Madaan, Eunho Yang, and Sung Ju Hwang. Online core-set selection for rehearsal-based continual learning. In *10th International Conference on Learning Representations, ICLR 2022*, 2022.
- [27] Rahaf Aljundi, Min Lin, Baptiste Goujaud, and Yoshua Bengio. Gradient based sample selection for online continual learning. *Advances in neural information processing systems*, 32, 2019.

- [28] Arslan Chaudhry, Ranzato Marc' Aurelio, Marcus Rohrbach, and Mohamed El-hoseiny. Efficient lifelong learning with a-gem. In *7th International Conference on Learning Representations, ICLR 2019*. International Conference on Learning Representations, ICLR, 2019.
- [29] P Dokania, P Torr, and M Ranzato. Continual learning with tiny episodic memories. In *Workshop on Multi-Task and Lifelong Reinforcement Learning*, 2019.
- [30] Yann Le and Xuan Yang. Tiny imagenet visual recognition challenge. *CS 231N*, 7(7):3, 2015.
- [31] Jonathan Schwarz, Wojciech Czarnecki, Jelena Luketina, Agnieszka Grabska-Barwinska, Yee Whye Teh, Razvan Pascanu, and Raia Hadsell. Progress & compress: A scalable framework for continual learning. In *International conference on machine learning*, pages 4528–4537. PMLR, 2018.
- [32] Friedemann Zenke, Ben Poole, and Surya Ganguli. Continual learning through synaptic intelligence. In *International conference on machine learning*, pages 3987–3995. PMLR, 2017.
- [33] Sylvestre-Alvise Rebuffi, Alexander Kolesnikov, Georg Sperl, and Christoph H Lampert. icarl: Incremental classifier and representation learning. In *Proceedings of the IEEE conference on Computer Vision and Pattern Recognition*, pages 2001–2010, 2017.
- [34] Arslan Chaudhry, Albert Gordo, Puneet Dokania, Philip Torr, and David Lopez-Paz. Using hindsight to anchor past knowledge in continual learning. In *Proceedings of the AAAI conference on artificial intelligence*, volume 35, pages 6993–7001, 2021.
- [35] Hyuntak Cha, Jaeho Lee, and Jinwoo Shin. Co2l: Contrastive continual learning. In *Proceedings of the IEEE/CVF International conference on computer vision*, pages 9516–9525, 2021.
- [36] Lucas Caccia, Rahaf Aljundi, Nader Asadi, Tinne Tuytelaars, Joelle Pineau, and Eugene Belilovsky. New insights on reducing abrupt representation change in

online continual learning. In *International Conference on Learning Representations*.

- [37] Fahad Sarfraz, Elahe Arani, and Bahram Zonooz. Sparse coding in a dual memory system for lifelong learning. In *Proceedings of the AAAI Conference on Artificial Intelligence*, volume 37, pages 9714–9722, 2023.
- [38] Kaiming He, Xiangyu Zhang, Shaoqing Ren, and Jian Sun. Deep residual learning for image recognition. In *Proceedings of the IEEE conference on computer vision and pattern recognition*, pages 770–778, 2016.
- [39] Chengqing Yu, Fei Wang, Zezhi Shao, Tangwen Qian, Zhao Zhang, Wei Wei, and Yongjun Xu. Ginar: An end-to-end multivariate time series forecasting model suitable for variable missing. In *Proceedings of the 30th ACM SIGKDD conference on knowledge discovery and data mining*, pages 3989–4000, 2024.
- [40] Ya-nan Han and Jian-wei Liu. Adaptive instance similarity embedding for online continual learning. *Pattern Recognition*, 149:110238, 2024.